Bol. Soc. Paran. Mat.
©SPM – E-ISSN-2175-1188
SPM: www.spm.uem.br/bspm

(3s.) **v. 2026 (44) 17** : 1–10.
ISSN-0037-8712
doi:10.5269/bspm.82365

# Influence of Magnetic Fields on Nanoparticle-Based Blood Flow in Arteries with Stenosis and Dilatation

M. Shiva Krishna and Maddileti Pasupula

ABSTRACT: Arterial stenosis refers to the pathological reduction in vessel diameter, which markedly diminishes blood circulation and plays a major role in cardiovascular diseases. Such constriction generates elevated tangential stresses that compromise arterial wall integrity, possibly leading to post-stenotic expansion or aneurysmal development. This study examines the flow behavior of blood containing suspended silver nanoparticles through an artery with a stenosed section followed by a dilated segment under an applied external field. Using the mild stenosis assumption, analytical expressions are derived for velocity distribution, pressure gradient, wall shear stress, and flow resistance. The influence of key physical parameters on hemodynamic quantities is explored. The stenosis height enhances impedance and wall stress, while enlarging the dilatation lowers them.

Keywords: Stenosis, dilatation, impedance, wall shear stress, nanoparticles, magnetic field.

## Contents

**1 Introduction** **1**

**2 Formulation of the Problem and its Solution** **2**
2.1 Geometry of the Problem . . . . . 2
2.2 Governing Equations . . . . . 3
2.3 Non-dimensionalization . . . . . 4
2.4 Analytical Solution . . . . . 5

**3 Results and Discussion** **6**

**4 Conclusion** **9**

## 1. Introduction

Stenosis is a vascular disorder defined by the progressive constriction of an artery, typically resulting from the accumulation of arteriosclerotic plaque or the growth of abnormal tissue within the arterial wall. This gradual accumulation encroaches upon the arterial lumen, thereby impeding normal blood flow. As the narrowing intensifies, it not only reduces the volume of blood that can pass through but also alters the pressure and velocity of the flow. Such disturbed flow patterns may induce elevated shear forces and localized turbulence, which may harm the endothelial cells lining the inner surface of the artery. Damage to these cells can further accelerate the growth of stenosis, creating a feedback loop where impaired flow worsens the narrowing, and the narrowing further disturbs the flow. The mutual interaction between altered hemodynamics and stenosis progression represents a key feature of vascular pathology.

Without timely diagnosis and intervention, stenosis progression may result in serious and potentially fatal outcomes. It can disrupt the normal functioning of the circulatory system by limiting the oxygen and nutrient supply to vital organs, potentially leading to complications such as ischemia, heart attacks, or strokes. Thus, understanding the mechanisms and effects of stenosis is essential for developing effective preventive and therapeutic strategies in cardiovascular medicine.

Investigating blood flow in stenosed arteries is essential, given that circulatory diseases contribute to more than 30% of worldwide mortality. Stenosis, the narrowing of arteries due to plaque or tissue growth, is a leading cause of such disorders. It restricts blood flow, disrupts normal cardiovascular function, raises blood pressure, and can damage vessel walls. This damage may lead to post-stenotic dilatation, where the artery expands abnormally beyond the narrowed region, increasing the risk of severe complications.

2020 *Mathematics Subject Classification:* 76Z05, 76W05, 92C35.
Submitted March 03, 2026. Published June 19, 2026.

Pioneering work on blood flow through stenosed arteries began with Young [9], who investigated the time-dependent effects of stenosis in a tubular flow system. Azuma and Fukushima [1] extended this by modeling flow patterns in stenosed vessels, while MacDonald [4] analyzed the impact of vascular stenosis under steady flow conditions. Subsequent researchers explored blood flow through mildly constricted tubes using both Newtonian and non-Newtonian fluid models under various physiological conditions. Notable contributions include studies by Shukla et al. [11], Chaturani and PonnalaguSamy [2], Tandon et al. (1993), Srinivasacharya and Srikanth (2008), and Bali and Awasthi (2012).

Stenotic dilatation is the abnormal widening of an artery that occurs just beyond a stenosed region. This condition is often observed in elderly individuals, particularly those with weakened nervous systems. When blood clots form and pressure builds up at a localized point, the arterial wall may begin to bulge outward. If this pressure continues to increase, it can lead to structural damage of the artery, potentially resulting in life-threatening complications.

Although the exact mechanisms behind post-stenotic dilatation are not fully understood, several factors have been proposed, including elevated lateral pressure, cavitation, abnormal shear stresses, and turbulence in blood flow. A deeper understanding of these contributing factors is crucial for improving the diagnosis and treatment of arterial diseases.

Several studies have explored the hemodynamic implications of post-stenotic dilatation. For example, Pincombe et al. [5] investigated how this phenomenon affects blood flow in stenosed coronary arteries. Priyadharshini and Ponalagusamy [8] modeled the flow of Herschel-Bulkley fluid in narrowed stenotic arteries with arterial dilatation. Prasad et al. [6] examined the influence of post-stenotic dilatation on the flow of couple stress fluids across narrowed arteries. Additionally, Sharma et al. [10] and Varma and Parihar (2009) studied the impact of a constant external magnetic field on multistage stenosis, and they observed that yield stress and stenosis decrease the wall shear stress and slow down the blood flow in regions affected by the magnetic field. Umadevi et al. [12] studied blood flow in an inclined artery with overlapping stenoses, considering magnetic field effects and the inclusion of copper nanoparticles. In recent years, numerous researchers have focused on analyzing the hemodynamic behaviour of blood flow in arteries affected by stenosis.

Inspired by the preceding studies, this research aims to analytically investigate how a narrow part and the wide part after it affect blood flow containing suspended silver nanoparticles under mild stenosis conditions. The study derives mathematical equations used to describe main flow properties such as velocity, flow resistance, as well as wall shear stress. The influence of multiple important variables on these blood flow properties is examined and illustrated through graphical representations, providing deeper insight into the hemodynamic behavior in stenosed arteries.

## 2. Formulation of the Problem and its Solution

### 2.1. Geometry of the Problem

The flow characteristics of an incompressible fluid are analyzed within an axisymmetric artery exhibiting mild stenosis accompanied by post-stenotic dilatations. The stenosis is assumed to develop symmetrically along the artery's axis. The shape of the arterial wall is illustrated in Figure 1.

The arterial wall geometry, originally proposed by Pincombe et al. [5], is expressed as follows:

$$h = \frac{R(z)}{R_0} = \begin{cases} 1 - \frac{\delta_i}{2R_0}\left[1 + \cos\left(\frac{2\pi}{l_i}\left(z - \alpha_i - \frac{l_i}{2}\right)\right)\right], & \text{for } \alpha_i \le z \le \beta_i, \\ 1, & \text{Otherwise} \end{cases} \tag{2.1}$$

Here $\delta_i$ denotes the extent to which the $i$th abnormal part extends in the arterial lumen of the blood vessel; positive values correspond to stenotic segments, whereas negative values indicate aneurysmal dilatations. $R$ denotes the arterial radius, while $R_0$ is the radius of healthy artery. The parameter $l_i$ corresponds to the length of the $i$th abnormal segment and $\alpha_i$ is the length from the starting point to where the $i$th abnormal segment begins and is given by

$$\alpha_i = \left(\sum_{j=1}^{i}(d_j + l_j)\right) - l_i$$

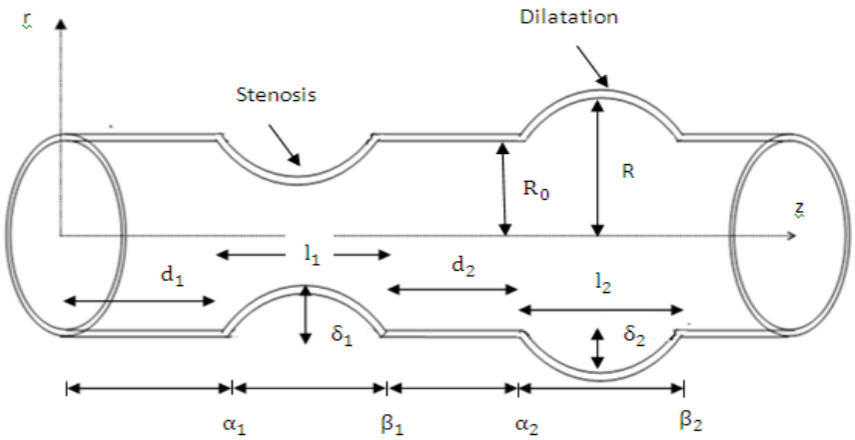


Figure 1: Schematic diagram of the tube with stenosis

and $\beta_i$ is the distance along the artery from the start to end of the $i$th abnormal segment

$$\beta_i = \left( \sum_{j=1}^{i} (d_j + l_j) \right)$$

where $d_i$ is the gap between starting point of the $i$th abnormal part and the end point of the $(i-1)$th part.

Relating to the works of Shukla et al. [11] and Maruthi Prasad and Radhakrishnamacharya [7], the assumptions for mild stenosis are considered under the following limitations:

$$\frac{\delta_i}{R_0} \ll 1, \quad \frac{L_i}{R_0} \ll 1$$

These conditions imply that $\delta_i$ is the height and length $L_i$ is the length of the stenosis are small compared to the normal arterial radius $R_0$.

### 2.2. Governing Equations

The equations governing the conservation of mass, momentum and temperature for an incompressible nanofluid can be considered as follows [13]:

$$\frac{\partial v}{\partial r} + \frac{v}{r} + \frac{\partial u}{\partial z} = 0 \tag{2.2}$$

$$\rho_{nf} \left( v \frac{\partial v}{\partial r} + u \frac{\partial v}{\partial z} \right) = -\frac{\partial p}{\partial r} + \mu_{nf} \frac{\partial}{\partial r} \left( 2 \frac{\partial v}{\partial r} \right) + \mu_{nf} \frac{\partial}{\partial z} \left( 2 \frac{\partial v}{\partial z} + \frac{\partial u}{\partial r} \right) \tag{2.3}$$

$$\rho_{nf} \left( v \frac{\partial u}{\partial r} + u \frac{\partial u}{\partial z} \right) = -\frac{\partial p}{\partial z} + \mu_{nf} \frac{\partial}{\partial z} \left( 2 \frac{\partial u}{\partial z} \right) + \mu_{nf} \frac{\partial}{\partial r} \left[ r \left( \frac{\partial v}{\partial z} + \frac{\partial u}{\partial r} \right) \right] - g \rho_{nf} \alpha (T - T_0) - \sigma B_0^2 u \tag{2.4}$$

$$v \frac{\partial T}{\partial r} + u \frac{\partial T}{\partial z} = \frac{k_{nf}}{(\rho c_p)_{nf}} \left( \frac{\partial^2 T}{\partial r^2} + \frac{1}{r} \frac{\partial T}{\partial r} + \frac{\partial^2 T}{\partial z^2} \right) + \frac{Q_0}{(\rho c_p)_{nf}} \tag{2.5}$$

with the boundary conditions

$$\frac{\partial u}{\partial r} = 0, \quad \frac{\partial T}{\partial r} = 0 \quad \text{at } r = 0 \tag{2.6}$$

$$u = 0, \quad T = 0 \quad \text{at} \quad r = h \tag{2.7}$$

Table 1: Thermophysical properties of blood and nanoparticles

| Physical properties | Blood | Ag |
|---|---|---|
| $C_p$ (J kg$^{-1}$ K$^{-1}$) | 3594 | 129 |
| $\rho$ (kg m$^{-3}$) | 1063 | 19320 |
| $k$ (W m$^{-1}$ K$^{-1}$) | 0.492 | 314 |
| $\sigma$ ($\Omega$ m)$^{-1}$ | $6.67 \times 10^{-1}$ | $4.1 \times 10^{7}$ |

In the above equations $u$ and $v$ represent the velocity components in the radial ($r$) and axial ($z$) directions, $T$ is the fluid temperature, $Q_0$ is the heat absorption constant, $\mu_{nf}$ is the effective viscosity, $\rho_{nf}$ is the density, $k_{nf}$ is the heat conductivity, $\alpha_{nf}$ is the heat diffusivity and $(\rho c_p)_{nf}$ is the heat capacity of fluid containing nanoparticles as shown below:

$$\mu_{nf} = \frac{\mu_f}{(1-\phi)^{2.5}}, \quad k_{nf} = k_f \left( \frac{k_s + 2k_f - 2\phi(k_f - k_s)}{k_s + 2k_f + 2\phi(k_f - k_s)} \right)$$

$$\rho_{nf} = (1-\phi)\rho_f + \phi\rho_s, \quad (\rho c_p)_{nf} = (1-\phi)(\rho c_p)_f + \phi(\rho c_p)_s$$

### 2.3. Non-dimensionalization

The following dimensionless variables are introduced:

$$\bar{r} = \frac{r}{R_0}, \quad \bar{z} = \frac{z}{L_0}, \quad \bar{v} = \frac{L_0}{\delta U} v, \quad \bar{u} = \frac{u}{U}, \quad \bar{d} = \frac{d}{L_0}, \quad \bar{R} = \frac{R}{R_0}$$

$$M^2 = \frac{\sigma B_0^2 R_0^2}{\mu_f}, \quad Gr = \frac{g\alpha R_0^2 T_0 \rho_{nf}}{U\mu_f}, \quad \delta = \frac{\delta}{R_0}, \quad \theta = \frac{T - T_0}{T_0}$$

$$\bar{p} = \frac{U L_0 \mu_f}{R_0^2} p, \quad \beta = \frac{Q_0 R_0^2}{k_f T_0}$$

where $U$ represents the average velocity across the tube cross-section, calculated over the area corresponding to a tube of radius $R_0$.

Applying the dimensionless variables in equations (2.2)–(2.5) and mild stenosis assumptions yields the reduced governing equations and associated boundary conditions:

$$\frac{\partial p}{\partial r} = 0 \tag{2.8}$$

$$\frac{\partial p}{\partial z} = \frac{1}{(1-\phi)^{2.5}} \frac{1}{r} \frac{\partial}{\partial r} \left( r \frac{\partial u}{\partial r} \right) - M^2 u + Gr\, \theta \tag{2.9}$$

$$\frac{1}{r} \frac{\partial}{\partial r} \left( r \frac{\partial \theta}{\partial r} \right) + \beta \left( \frac{k_{nf}}{k_f} \right) = 0 \tag{2.10}$$

Here $M$, $\beta$ and $Gr$ are the Hartmann number, heat absorption parameter and the Grashof number respectively.

The boundary conditions become:

$$\frac{\partial u}{\partial r} = 0, \quad \frac{\partial \theta}{\partial r} = 0 \quad \text{at } r = 0 \tag{2.11}$$

$$u = 0, \quad \theta = 0 \quad \text{at } r = h \tag{2.12}$$

### 2.4. Analytical Solution

The solutions of equations (2.9) and (2.10) subject to boundary conditions (2.11)–(2.12) are as follows:

**Theorem 2.1** *The dimensionless velocity distribution is given by*

$$u = \left\{ \frac{1}{M^2}\frac{dp}{dz} - \frac{Gr\,\beta}{M^2}\left(\frac{k_f}{k_{nf}}\right)\right\}\left[1 - \frac{I_0\left(Mr\sqrt{(1-\phi)^{2.5}}\right)}{I_0\left(Mh\sqrt{(1-\phi)^{2.5}}\right)}\right] - \frac{Gr\,\beta}{4M^2}\left(\frac{k_f}{k_{nf}}\right)(r^2-h^2) - \frac{1}{M^2}\frac{dp}{dz} + \frac{Gr\,\beta}{M^2}\left(\frac{k_f}{k_{nf}}\right) \tag{2.13}$$

**Theorem 2.2** *The dimensionless temperature distribution is given by*

$$\theta = -\frac{\beta}{4}\left(\frac{k_f}{k_{nf}}\right)(r^2-h^2) \tag{2.14}$$

The dimensionless flux $Q$ is

$$Q = 2\int_0^h ru\,dr$$

Evaluating this integral yields:

$$Q = \left(\frac{1}{M^2}\frac{dp}{dz} - \frac{Gr\,\beta}{M^2}\left(\frac{k_f}{k_{nf}}\right)\right)\left(\frac{hI_1\left(Mh\sqrt{(1-\phi)^{2.5}}\right)}{M\sqrt{(1-\phi)^{2.5}}\,I_0\left(Mh\sqrt{(1-\phi)^{2.5}}\right)}\right) + \frac{Gr\,\beta}{16M^2}\left(\frac{k_f}{k_{nf}}\right) - \frac{Gr\,\beta h^2}{2M^2}\left(\frac{k_f}{k_{nf}}\right) - \frac{h^2}{M^2}\frac{dp}{dz}$$

This implies

$$\frac{dp}{dz} = \frac{\dfrac{Gr\,\beta}{16M^2}\left(\dfrac{k_f}{k_{nf}}\right) - \dfrac{Gr\,\beta h^2}{2M^2}\left(\dfrac{k_f}{k_{nf}}\right) + \dfrac{Gr\,\beta}{M^2}\left(\dfrac{k_f}{k_{nf}}\right)\left(\dfrac{hI_1\left(Mh\sqrt{(1-\phi)^{2.5}}\right)}{M\sqrt{(1-\phi)^{2.5}}\,I_0\left(Mh\sqrt{(1-\phi)^{2.5}}\right)}\right)}{\dfrac{h^2}{M^2} - \dfrac{h^3}{2M^2}\left(\dfrac{I_1\left(Mh\sqrt{(1-\phi)^{2.5}}\right)}{I_0\left(Mh\sqrt{(1-\phi)^{2.5}}\right)\sqrt{(1-\phi)^{2.5}}}\right)} \tag{2.15}$$

**Definition 2.1** *Flow resistance $\lambda$ is defined as*

$$\lambda = \frac{\Delta p}{Q} = \int_0^1 \frac{dp}{dz}\,dz \tag{2.16}$$

Pressure drop without stenosis ($h = 1$) is defined as

$$\Delta p_n = \left[\int_0^1 \frac{dp}{dz}\,dz\right]_{h=1} \tag{2.17}$$

Flow resistance in the normal artery is defined as

$$\lambda_n = \frac{\Delta p_n}{Q} \tag{2.18}$$

Normalized flow resistance is defined as

$$\bar{\lambda} = \frac{\lambda}{\lambda_n} \tag{2.19}$$

**Definition 2.2** *Wall shear stress $\tau_h$ is defined as*

$$\tau_h = -\frac{h}{2}\frac{dp}{dz} \tag{2.20}$$

## 3. Results and Discussion

The blood resistance flow and wall shear stress on the vessel wall are two critical parameters in blood flow analysis in a stenotic artery with post-stenotic dilatation. Analytical expressions for the fluid velocity ($u$), flow resistance ($\lambda$) and wall shear stress ($\tau_h$) are provided by equations (2.13), (2.16), and (2.20), respectively. The individual effects of various physical and geometric parameters on $\lambda$ and $\tau_h$ are investigated numerically using Mathematica, and the results are illustrated graphically to provide insight into the hemodynamic behavior under different conditions.

Figures 2–4 depict the variation of resistance flow with respect to the height of stenosis and dilatation ($\delta_1$ and $\delta_2$), Hartmann number ($M$), Grashof number ($G_r$), flow rate ($Q$), and heat absorption constant ($\beta$). It has been noticed that the flow resistance ($\lambda$) rises with increasing stenosis heights ($\delta_1$), Hartmann number ($M$), Grashof number ($G_r$), and heat absorption constant ($\beta$) but drops with the height of dilatation ($\delta_2$) and rate of flow ($Q$).

It has been found that there is a reduction in flow resistance when silver nanoparticles are introduced into the blood, as compared to the case with pure blood. This is primarily due to the improved thermal conductivity of the nanoparticle-suspended fluid, which enhances heat transfer within the artery. The resulting rise in temperature leads to a decrease in the fluid's viscosity, thereby promoting smoother flow and lowering resistance through the stenosed region.

The variation of wall shear stress ($\tau_h$) with respect to stenosis height and post-stenotic dilatation height, under different values of the Hartmann number ($M$), Grashof number ($G_r$), and heat absorption coefficient ($\beta$), is illustrated in Figures **??**–**??**. It is noticed that shear stress ($\tau_h$) increases with height of the stenosis ($\delta_1$) and flow rate ($Q$), indicating greater resistance near the constricted region. In contrast, $\tau_h$ diminishes as the Hartmann number ($M$), Grashof number ($G_r$), and heat absorption parameter ($\beta$) increase, due to their damping effects on the flow rate. Additionally, the shear force on the vessel wall is found to increase with the inclusion of silver nanoparticles, owing to their influence on enhancing thermal conductivity and modifying the rheological properties of the fluid.

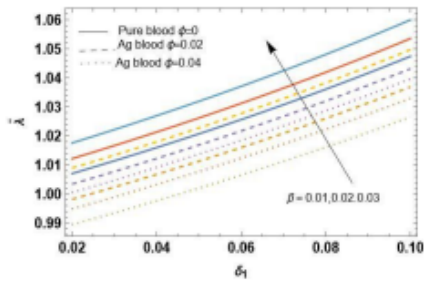


Fig. 2. Diagram of $\delta_1 \& \beta$ on $\bar{\lambda}$ with $d_1 = d_2 = 0.2, L_1 = L_2 = 0.2$, $G_r = 0.2, \delta_2 = 0.02, M = 1, Q = 0.01$.

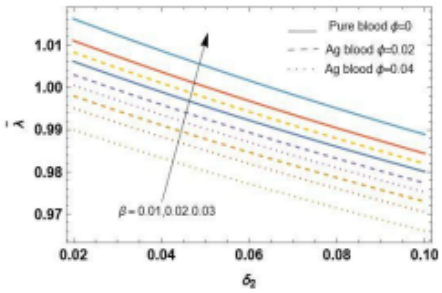


Fig. 3.Diagram of $\delta_2 \& \beta$ on $\bar{\lambda}$ with $d_1 = d_2 = 0.2, L_1 = L_2 = 0.2$, $G_r = 0.2, \delta_1 = 0.02, Q = 0.01, M = 1$.

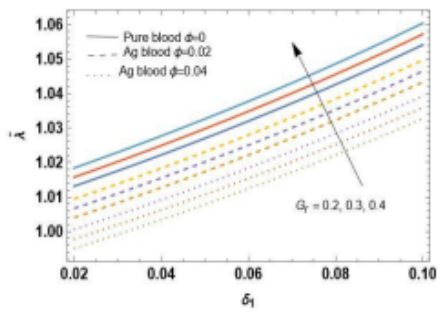


Fig. 4.Diagram of $\delta_1 \& \beta$ on $\bar{\lambda}$ with $d_1 = d_2 = 0.2, L_1 = L_2 = 0.2$, $Q = 0.01, \delta_2 = 0.02, \beta = 0.01, M = 1$

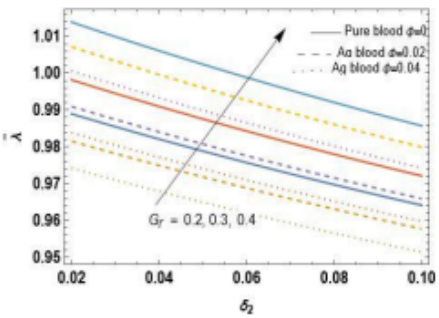


Fig. 5.Diagram of $\delta_2 \& \beta$ on $\bar{\lambda}$ with $d_1 = d_2 = 0.2, L_1 = L_2 = 0.2$, Q=0.01 $\delta_1 = 0.02, \beta = 0.01, M = 1$.

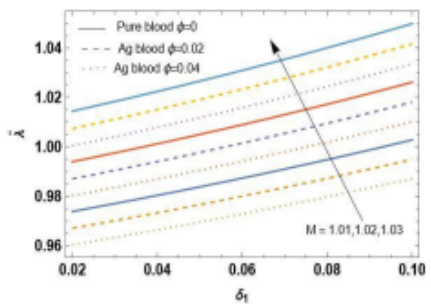


Fig. 6.Diagram of $\delta_1 \& \beta$ on $\bar{\lambda}$ with $d_1 = d_2 = 0.2, L_1 = L_2 = 0.2$, $Q = 0.01, G_r = 0.2, \delta_2 = 0.02, \beta = 0.01$.

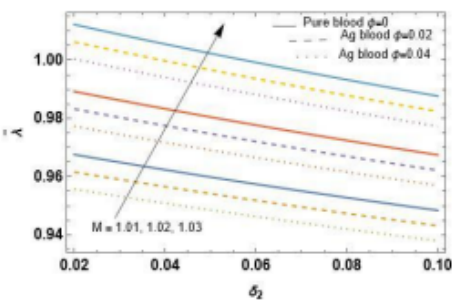


Fig. 7.Diagram of $\delta_2 \& \beta$ on $\bar{\lambda}$ with $d_1 = d_2 = 0.2, L_1 = L_2 = 0.2$, Q = 0.01 $G_r = 0.2, \delta_1 = 0.02, \beta = 0.01$.

Figure 2: Effect of parameters on flow resistance

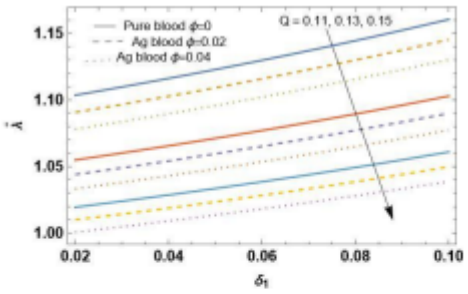


Fig. 8.Diagram of $\delta_1$&$\beta$ on $\bar{\lambda}$ with $d_1 = d_2 = 0.2, L_1 = L_2 = 0.2$, $G_r = 0.2, \delta_2 = 0.02, M = 1, \beta = 0.01$.

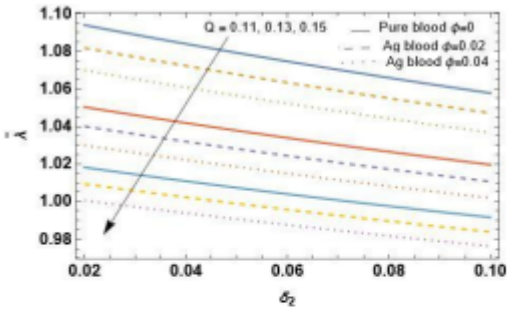


Fig. 9.Diagram of $\delta_2$&$\beta$ on $\bar{\lambda}$ with $d_1 = d_2 = 0.2, L_1 = L_2 = 0.2$, $G_r = 0.2, \delta_1 = 0.02, M = 1, \beta = 0.01$.

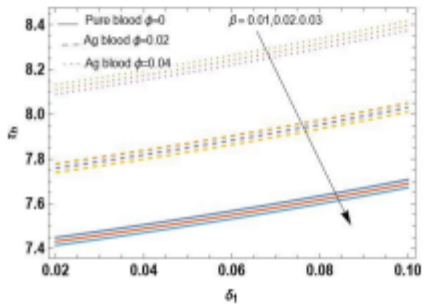


Fig. 10.Diagram of $\delta_1$ &$\beta$ on $\tau_h$ with $d_1 = d_2 = 0.2, L_1 = L_2 = 0.2$, $G_r = 0.2, \delta_2 = 0.02, Q = 0.1, M = 1$.

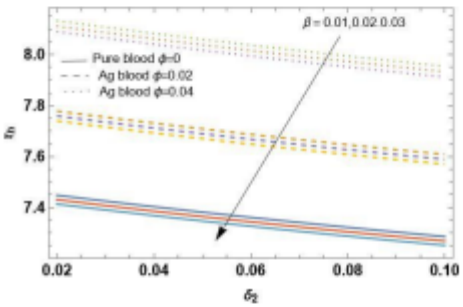


Fig. 11.Diagram of $\delta_2$&$\beta$ on$\tau_h$ with $d_1 = d_2 = 0.2, L_1 = L_2 = 0.2$, $G_r = 0.2, \delta_1 = 0.02, M = 1, Q = 0.1$.

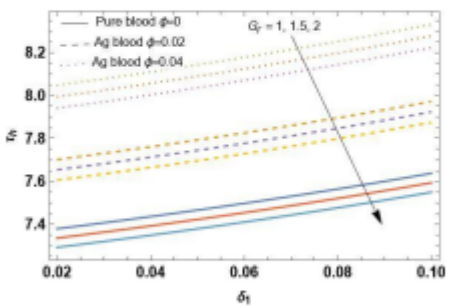


Fig. 12.Diagram of $\delta_1$ & $G_r$ on $\tau_h$ with $d_1 = d_2 = 0.2, L_1 = L_2 = 0.2$, $\delta_2 = 0.02, Q = 0.1, M = 1, \beta$ −0.01

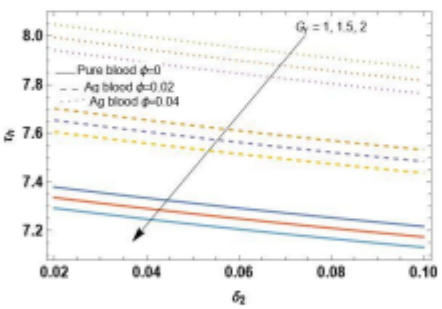


Fig. 13.Diagram of $\delta_2$& $G_r$ on$\tau_h$ with $d_1 = d_2 = 0.2, L_1 = L_2 = 0.2$, $\delta_1 = 0.02, M = 1, Q = 0.1, \beta$ −0.01.

Figure 3: Effect of parameters on flow resistance (continued)

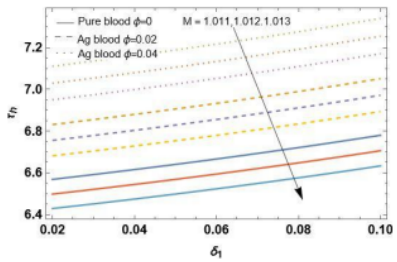


Fig. 14.Diagram of $\delta_1$ &$M$ on $\tau_h$ with $d_1 = d_2 = 0.2, L_1 = L_2 = 0.2,$ $\delta_2 = 0.02, Q = 0.1, G_r = 0.2, \beta$ =0.01

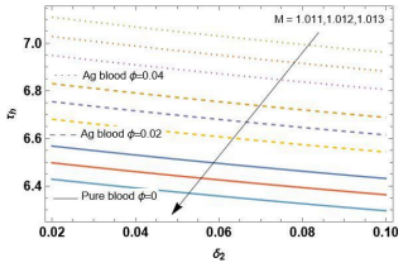


Fig. 15.Diagram of $\delta_2$&$M$ on$\tau_h$ with $d_1 = d_2 = 0.2, L_1 = L_2 = 0.2,$ $\delta_1 = 0.02, Q = 0.1, G_r = 0.2, \beta$ =0.01.

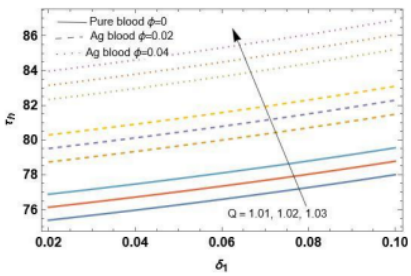


Fig. 16.Diagram of $\delta_1$ &$M$ on $\tau_h$ with $d_1 = d_2 = 0.2, L_1 = L_2 = 0.2,$ $\delta_2 = 0.02, G_r = 0.2, \mathrm{M} = 1, \beta$ =0.01

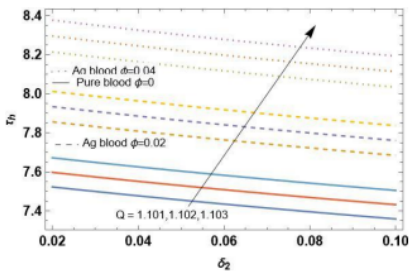


Fig. 17.Diagram of $\delta_2$&$M$ on $\tau_h$ with $d_1 = d_2 = 0.2, L_1 = L_2 = 0.2,$ $\delta_1 = 0.02, G_r = 0.2, \mathrm{M} = 1, \beta$ =0.01.

Figure 4: Effect of parameters on flow resistance (continued)

## 4. Conclusion

The present study focuses on the inclusion of silver nanoparticles in the base fluid for the axisymmetric blood flow with stenosed artery and dilatation. In this work we studied the effects of several parameters like heights of the stenosis and dilatation, Grashof number, heat absorption constant and Hartmann number on blood flow characteristics, flow resistance and shear stress.

The following conclusions are drawn:

1. The flow resistance rises with the heights of the stenosis, Hartmann number, Grashof number, and heat absorption constant but decreases with the height of dilatation and flow rate.

2. An increase in wall shear stress is observed with greater stenosis severity and higher flow rates, indicating greater resistance near the constricted region. Conversely, it decreases with an increase in the Hartmann number, Grashof number, and heat absorption constant.

## Acknowledgments

The authors acknowledge the support and facilities provided by their respective institutions.

## References

1. T. Azuma and T. Fukushima, *Flow patterns in stenotic blood vessel models*, Biorheology 13, 337–355, (1976).

2. P. Chaturani and R. Ponnalagusamy, *Pulsatile flow of Casson's fluid through stenosed arteries with applications to blood flow*, Biorheology 23, 499–511, (1986).

3. J. H. Forrester and D. F. Young, *Flow through a converging–diverging tube and its implications in occlusive vascular disease*, Journal of Biomechanics 3, 297–316, (1970).

4. D. A. MacDonald, *On steady flow through modelled vascular stenosis*, Journal of Biomechanics 12, 13–30, (1979).

5. B. Pincombe, B. Mazumdar, and J. Hamilton-Craig, *Effects of multiple stenoses and post-stenotic dilation on non-Newtonian blood flow in small arteries*, Medical & Biological Engineering & Computing 37, 595–599, (1999).

6. K. M. Prasad, T. Sudha, and M. V. Phanikumar, *The effects of post-stenotic dilatation on the flow of couple stress fluid through stenosed arteries*, American Journal of Computational Mathematics 6, 365–376, (2016).

7. M. K. Prasad and G. Radhakrishnamacharya, *Flow of Herschel–Bulkley fluid through an inclined tube of non-uniform cross-section with multiple stenosis*, Archive of Mechanics 60, 161–172, (2008).

8. S. Priyadharshini and R. Ponnalagusamy, *Biorheological model on flow of Herschel–Bulkley fluid through a tapered arterial stenosis and dilatation*, Applied Bionics and Biomechanics, Article ID 406195, 1–12, (2015).

9. D. F. Young, *Effects of a time-dependent stenosis on flow through a tube*, Journal of Engineering for Industry 90, 248–254, (1968).

10. M. K. Sharma, P. R. Sharma, and V. Nasha, *Pulsatile MHD arterial blood flow in the presence of double stenosis*, Journal of Applied Fluid Mechanics 6(3), 331–338, (2013).

11. J. B. Shukla, R. S. Parihar, and B. R. P. Rao, *Effects of stenosis on non-Newtonian flow through an artery with mild stenosis*, Bulletin of Mathematical Biology 42, 283–294, (1980).

12. C. Umadevi, M. Dhange, B. Haritha, and T. Sudha, *Flow of blood mixed with copper nanoparticles in an inclined overlapping stenosed artery with magnetic field*, Case Studies in Thermal Engineering 25, Article ID 100947, (2021).

13. N. S. Akbar and W. Butt, *Magnetic field effects for copper suspended nanofluid flow through composite stenosed arteries with permeable walls*, Journal of Magnetism and Magnetic Materials, 1–7, (2015).

14. F. Tang et al., *Nanofluid flow analysis in stenosed arteries*, Case Studies in Thermal Engineering 47, Article ID 103064, (2023).

*M. Shiva Krishna,*
*Department of Mathematics,*
*TKR College of Engineering & Technology,*
*Meerpet, Hyderabad, India.*

*and*

*Maddileti Pasupula,*
*Department of Mathematics,*
*Mahatma Gandhi University,*
*Nalgonda, Telangana, India.*
*E-mail address:* marrishivakrishna@gmail.com, madhu.june5@gmail.com